Research in Pharmaceutical Sciences, June 2022; 17(3): 252-264
Received: 08-12-2021
Peer Reviewed: 04-01-2022
Revised: 14-01-2022
Accepted: 16-02-2022
Published: 18-04-2022

School of Pharmacy & Pharmaceutical Sciences
Isfahan University of Medical Sciences

Original Article

Synthesis, characterization, molecular docking, antimalarial, and antiproliferative activities of benzyloxy-4-oxopyridin benzoate derivatives

Marjan Mohebi[1,2], Neda Fayazi[3,4], Somayeh Esmaeili[3], Mahboubeh Rostami[1], Fereshteh Bagheri[2], Alireza Aliabadi[2], Parvin Asadi[1], and Lotfollah Saghaie[1,*]

[1]Department of Medicinal Chemistry, School of Pharmacy and Pharmaceutical Sciences, Isfahan University of Medical Sciences, Isfahan, I.R. Iran.
[2]Pharmaceutical Sciences Research Center, Health Institute, Kermanshah University of Medical Sciences, Kermanshah, I.R. Iran.
[3]Traditional Medicine and Materia Medica Research Center (TMRC), School of Traditional Medicine, Shahid Beheshti University of Medical Sciences, Tehran, I.R. Iran.
[4]Phytochemistry Research Center, School of Pharmacy, Shahid Beheshti University of Medical Sciences, Tehran, I.R. Iran.

Abstract

Background and purpose: Malaria and cancer are two major health issues affecting millions of lives annually. Maltol complexes and derivatives have been extensively investigated as chemotherapeutic and antimalarial activities. In this study, the design, synthesis, biological activities, and docking study of a novel series of pyridinones derivatives were reported.

Experimental approach: The chemical structures of synthesized compounds were approved by FTIR, ^{1}HNMR, ^{13}CNMR, and mass spectroscopies. The antimalarial activity was evaluated through β-hematin inhibition assay and the cytotoxicity activities were evaluated against PC12 and fibroblast cell lines via MTT and cell uptake assays. To theoretically investigate the ability of compounds to inhibit hemozoin formation, the synthesized compounds were docked in a heme sheet to explore their binding mode and possible interactions.

Findings/Results: β-Hematin inhibition assay showed acceptable activity for **7f, 7c,** and **7d** compounds and the molecular docking study showed **7h** and **7f** had effective interactions with the heme sheet. The cytotoxic study revealed compound **4b** (IC_{50} = 18 µM) was significantly more active against PC12 cells than docetaxel (IC_{50} = 280 µM). The observations of cell uptake images were also shown both cell penetration and monitoring potential of synthesized compounds.

Conclusion and implications: The compounds showed a moderate ability to inhibition of heme polymerization and also good interaction with heme through molecular docking was observed. Additionally, some of them have a good cytotoxic effect on the study2 cell line. So further study on these compounds can lead to compounds that can be considered as anti-malarial and/or anticancer agents.

Keywords: Antimalarial activity; Anti-proliferative assay; β-hematin, Pyridinone derivatives.

INTRODUCTION

Malaria and cancer are two major health issues affecting millions of lives annually. Malaria is a global health challenge induced by the microparasite of the *Plasmodium* ilk, *P. falciparum*, and resulted in approximately 2 million annual deaths, especially in children under the age of five (1).

* Corresponding author: L. Saghaie
Tel: +98-3137927098, Fax: +98-3136680011
Email: saghaie@pharm.mui.ac.ir

Access this article online

Website: http://rps.mui.ac.ir

DOI: 10.4103/1735-5362.343079

A major problem about malaria is the rapid appearance and spread of resistant strains across endemic areas which makes the current antimalarial drugs such as the quinine family and antifolate pyrimethamine inactive and require the search for new chemotherapeutic agents (2, 3).

One strategy to control malaria infections is disruption of the parasite life cycle in the host body (4). Inhibition of hemozoin formation is a validated strategy for most of the well-known existing antimalarial drugs and is considered an appropriate target to develop new antimalarials (4,5).

Contrary to malaria, which is an infectious disease, cancer is a non-communicable disease, ranking as the second leading cause of death globally, responsible for approximately 1 in 6 deaths. Current cancer treatments are surgery, chemotherapy, and radiation therapy (6). Among the three treatments, the most powerful approach to kill the cancer cells that have spread is the use of synthetic drugs through chemotherapy. However, this specific treatment can also lead to treatment failure and the development of cancer (7). Several types of cancer cells have exhibited resistance to current chemotherapeutic drugs such as cisplatin, therefore new anticancer drugs are needed to fight cancer (8).

Maltol as a member of the 2-alkyl-3-hydroxy4-pyrones family is a naturally occurring compound and exhibits many practical applications primarily in the food, cosmetic, and pharmaceutical industry (9). Maltol is used in drugs such as ferric trimaltol for the treatment of iron deficiency anemia and vanadylmaltolate for the treatment of diabetes (10). This compound is a promising polyfunctional heterocyclic skeleton with several important centers enabling additional reactions like alkylation, acylation, oxidation, nucleophilic, and electrophilic substitution reduction, Michael addition, and chelation are often used as desired procedures in the synthesis of many other biologically active agents (11). Maltol is known for its antioxidative properties (12) and its ability to chelate metal ions (13). It is an effective ligand for increasing absorption and bioavailability of metal ions (14) to combat widespread multiple drug resistance in human malaria. The effect of maltol was also investigated on the growth of *P. falciparum* in a series of experiments (15). Maltol inhibited the growth of *P. falciparum* by about 15% and 50% at 0.01 mM and 0.10 mM, compared to control, respectively (15). These findings made the hydroxyl pyridinone scaffold a good candida for antimalarial agents and the synthesis of different derivatives showed that increased affinity to iron as well as increased lipophilicity may improve antimalarial activity (16). On the other hand, maltol can improve immune functions, induce apoptosis, and inhibit angiogenesis, consequently suppressing the tumor growth of H22 transplanted tumors (17). Furthermore, maltol complexes and derivatives have been extensively investigated in the past decades as chemotherapeutic agents against cancer and some of them were found to have significant cytotoxicity towards human cancer cell lines (IC_{50} below 10 μm) (11,18,19).

Considering the aforementioned facts and in continuation of our previous findings on the biological activity of maltol derivatives (20), in the current study, we are interested in further exploring the biological activities of some novel maltol derivatives to provide new leads for antimalarial and/or anticancer drug development studies. Here, the use of maltol is not due to its iron-chelating properties, but it has been used as a moiety that can prevent the formation of beta-homozygous through hydrophobic interaction with heme. Therefore in this work, the benzyl groups in the structure were preserved and the debenzylation reaction will not be performed. After structural confirmation of novel synthesized derivatives, we examined the compounds for antimalarial and cytotoxic activity through standard related protocol and the structure-activity relationships discussed by introducing different substituents at benzoate ring on their antimalarial and cytotoxic activities.

MATERIALS AND METHODS

All reagents were procured from Merck and Sigma-Aldrich (Germany) and used without extra purification, except dichloromethane stored on a molecular sieve. Thin-layer chromatography (TLC, silica-gel 60 F_{254} plates,

Merck) was employed for monitoring the reaction. Proton and carbon-13 nuclear magnetic resonance (^{1}H NMR and ^{13}C NMR) spectra were assigned on a Varian-INOVA spectrometer (500 MHz), running at ambient probe temp. Chemical shifts (δ) were stated in ppm. $Si(CH_3)_4$, was applied as the internal standard. Direct mass spectrometry (MS) was recorded using an Agilent 5975C operating with an EI source. The uncorrected melting point was measured on the electrothermal melting point apparatus. Fourier transform infrared (FT-IR) spectra (Shimadzu IR, USA) was recorded in the range of 400-4000 cm^{-1}.

Synthesis of 3-(3-(benzyloxy)-2-methyl-4-oxopyridin-1(4H)-yl) propyl benzoate derivatives

The synthesized 3-(3-(benzyloxy)-2-methyl-4-oxopyridin-1(4H)-yl) propyl benzoate derivatives (**7a-7h**) were prepared as illustrated in Scheme1.

Synthesis of the 3-(benzyloxy)-2-methyl-4H-pyran-4-one (3)

A 250 mL double-necked round-bottomed flask that fitted with a magnetic mixer was charged with maltol (6.3 gr, 50 mmol), methanol (60 mL), and aqueous NaOH (5 mL, 11 M), followed by the dropwise addition of benzyl chloride (6.33 mL, 50 mmol), then the reaction was mixed and refluxed overnight. After finalization of the reaction, the solvent was removed by rotary evaporation, the crude product was washed by 5% aqueous NaOH (2 × 50 mL) and water (2 × 50 mL). Then, the resulting mixture was extracted with dichloromethane (3 × 50 mL), the organic portion was dried over anhydrous $MgSO_4$ and filtered out. The solvent was removed by rotary evaporation to give a brown oil, which was sprinkled with diethyl ether, cooled at 0 °C, gave compound **3** as pure needle-shaped crystals (21).

Synthesis of 3-(benzyloxy)-1-(3-hydroxypropyl)-2-methylpyridin-4(1H)-one (4)

To preparation of precursor **(4)**, benzylmaltol **(3)** (1 g, 4.6 mmol) in water/ethanol (50/50), and 3-amino-1-propanol (0.6 g, 8 mmol) were mixed and sodium hydroxide solution (5%) was added to adjust pH 13. The reaction was refluxed overnight and then the pH of the reaction mixture was adjusted to 7 with hydrochloric acid (6 M) and extracted with dichloromethane (3 × 50 mL). The organic layer was extracted, dried over anhydrous $MgSO_4$, sieved, and concentrated to give compound **4** as a pure brownish oil (21).

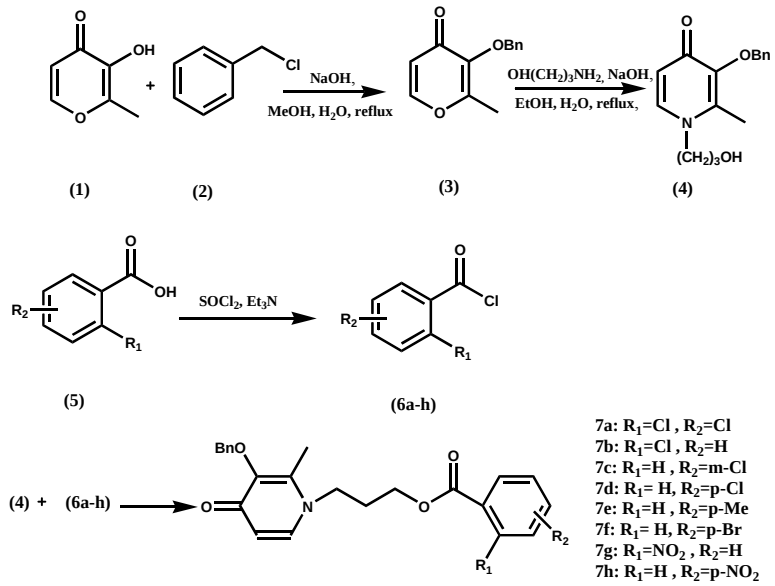

Scheme 1. Synthesis steps of 3-(3-(benzyloxy)-2-methyl-4-oxopyridin-1(4H)-yl) propyl benzoate derivatives.

General procedure synthesis of benzoyl chloride derivatives (6a-6h)

To synthesize benzoyl chloride derivatives, triethylamine as a catalyst was added to a stirring suspension of 4-chlorobenzoic acid derivatives (8 mmol) in dichloromethane (50 mL). Then, thionyl chloride (0.6 mL, 8. mmol) was added to the mixture at 0 °C and the reaction was stirred for completion. After completion of reaction through checking by TLC, the solvent was evaporated under vacuum, and the desired compounds were purified through washing with cold n-hexane.

General procedure synthesis of 3-(3-(benzyloxy)-2-methyl-4-oxopyridin-1(4H)-yl) propyl benzoate derivatives (7a-7h)

For the synthesis of final compounds, 4 mmol (1 g) of compound **4** was dissolved in dichloromethane in presence of triethylamine (4 mmol, 0.56 mL) and then, added to benzoyl chloride derivatives. Afterward, the solution was stirred at room temperature for 48 h. Upon completion, the resulting mixture was concentrated under vacuum to yield the crude product, which was prewashed with water and then purified TLC using a mixture EtOAc/petroleum ether 9:1 (v/v) as eluent.

In vitro ß-hematin inhibition assay

Bioassay was carried out by the inhibition test of heme detoxification (ITHD) method (22). The test was carried out at hemin concentrations (30, 60, 120 µM), pHs (3.6, 4, 4.4, 4.8, and 5) at 37 °C, 60 °C three times (4, 24, 48 h). Bioassay procedure was as follows, hemin chloride was dissolved in dimethyl sulfoxide (DMSO) diluted to 60 µg/mL by sodium acetate buffer (1 M, pH = 4.5), instead of β-hematin, hemin was employed in acidic condition (acetate buffer), Tween® 20 was diluted to 0.012 g/L with distilled water and synthesized compounds were dissolved by DMSO. Hemin, samples, and Tween® 20 were distributed in each well of a 96-well plate with a ratio of 9:9:2, respectively, in triplicate. The final concentration of all the materials in each well was 200 µg/mL (22).

As a control, these samples were prepared in triplicate under the same condition in lack of hemin. These controls allowed being prevented interference absorption of those remains from matrix samples. Negative control samples were dissolved in DMSO without hemin. Chloroquine phosphate was used as a positive control. The plates were incubated at 60 °C for 24 h. Finally, the materials in plates were mixed with a micropipette and then adsorption of the solutions was read at 405 nm by ELISA reader (Epoch, BioTeK, USA).

In vitro antiproliferative assay

Cytotoxicity of synthesized compounds was studied against PC12 derived from a pheochromocytoma of the rat adrenal medulla (C153) and fibroblast (C646) cells through the MTT method (23). For this purpose, the cell lines were obtained from the Institute of Pasteur, Tehran, Iran. The cell-cultured in 5000 cells per well of PC12 and fibroblast cells were separately cultured with Dulbecco's modified essential medium (DMEM) containing 10% heat-inactivated fetal bovine serum (FBS), penicillin (100 U/mL), and streptomycin (100 µg/mL) in 96-well plates, incubated for 24 h. Then, the confluence of cells reached 80% of the appropriate concentrations of each compound, docetaxel, and cisplatin as positive controls (1, 5, 10, 20, 40, 80, 120, and 360 µg/mL) were added to each well and incubated for 48 h. After this time, 10% of MTT solution (5 mg/mL in PBS buffer pH 7.4) was added to each well and incubated for another 3-4 h. The supernatants of the wells were then removed and 100 µL of DMSO was added to each of them to solubilize formazan crystals. Finally, the absorbance of each well was read at 570 nm using an ELISA reader (Bio-rad. USA). The IC_{50} values were calculated by a Graphpad prism 6 version and Excel software, 16 version

Cellular uptake of target compounds

Neuronal PC12 cancer cell line at a density of 5×10^4 cells/well in a 6-well plate was cultured in DMEM supplemented with 10% FBS and antibiotics. The culture was maintained in a 95% air humidified atmosphere containing 5% CO2 at 37 °C. The cells were incubated with 50 and 100 µM/mL synthesized compounds at 37 °C for 24 h, the medium removed, washed with cold PBS three times, and then washed with

sterilized distilled water for 3 min (24). Finally, the pictures of fluorescent emission of treated and non-treated cells were recorded by fluorescent microscope (BioTekTM CytationTM 1 Cell Imaging Multi-Mode Reader, USA)

Molecular docking

Structure-based evaluation is a usual method for the prediction of receptor-ligand interactions in the drug development process. Docking studies were performed using the Gold 5.3 program (The Cambridge Crystallographic Data Center, Cambridge, UK). The structures of synthesized compounds were built using the ChemDraw program and then transferred into Discovery Studio 4.1 (AccelrysInc, San Diego, CA, USA). Ligand structures were typed with CHARMm force field and partial charges were calculated by the Momany-Rone option (25). Then, they were minimized with Smart Minimizer which performs 1000 steps of steepest descent with a root mean square (RMS) gradient tolerance of 3 and conjugate gradient minimization (26). The crystal structure of heme was taken from RCSB Protein Data Bank (ID: E529). GOLD utilizes a genetic algorithm for conformational search and molecular docking. As a result, 10 ligand conformations were obtained and were ranked according to the GOLD fitness function. Finally, the best poses were chosen for binding analysis (27).

RESULTS

Characterization of synthesized compounds

3-(benzyloxy)-2-methyl-4H-pyran-4-one (3)

Needle crystals; yield 8.7 g (80%); mp 53-54 °C (21); IR (cm^{-1}): 1647 (C=O), 1577 (C=C).

3- (benzyloxy) -1- (3- hydroxypropyl) -2-methylpyridin-4(1H)-one (4)

Brownish oil; yield 1.1 g (87%); IR (cm^{-1}): 3329 (broad strong O-H stretch), 1627 (ketone C=O stretch), 1261 (C-O stretching), 2873-2924 (C-H, aliphatic, stretching), 1338 (C-N stretching), 1261 (C-O stretching) 3070 (aromatic C-H stretching) ,1519 (C=C, aromatic, bending), 2873-2924 (C-H, aliphatic, stretching). ^{1}H NMR ($CDCl_3$, 500 MHz) δ (ppm) 1.72 (m, 2H, N-CH_2*CH_2* CH_2), 2.01 (s, 3H, 2-*CH_3*), 3.51 (t, 2H, N*CH_2*CH_2), 3.63-3.71 (br, 1H, OH), 3.90 (t, 2H, CH_2*CH_2*O), 5.02 (s, 2H,*CH_2*ph), 6.31 (d, 1H, 5-*H*(pyridinone)), 7.22-7.32 (m, 6H, *Ar* and *6-H*(pyridinone)). ^{13}C NMR ($CDCl_3$, 500 MHz) δ (ppm) 12.3, 32.9, 50.7, 57.4, 73.1, 116.6, 128.1, 128.3, 128.9, 137.3, 139.3, 141.9 145.9, 173.2. MS: *m/z* 273 $[M]^+$ (21).

3- (3- (benzyloxy)-2-methyl -4-oxopyridin-1(4H)-yl) propyl 2, 4-dichlorobenzoate (7a)

Light brownish oil; yield 0.97 g (55%); IR (cm^{-1}): 1732 (ester C=O stretch), 1625 (α, β-unsaturated ketones C=O stretch), 1354 (C-N stretching), 1251-1290 (C-O stretching), 3066 (aromatic C-H stretching), 837 (aromatic weak CH out-of-plane bending modes), 2854-2926 **(**C-H, aliphatic, stretching), 1533 (C=C, aromatic, bending) ^{1}H NMR ($CDCl_3$, 500 MHz) δ (ppm) 2.00-2.10 (br, 5H, N-CH_2*CH_2*CH_2O and *2-CH_3*), 3.90 (t, 2H, N*CH_2*CH_2), 4.31 (t, 2H, CH_2*CH_2*O), 5.20 (s, 2H,*CH_2*ph), 6.52 (d, 1H, *5-H* (pyridinone)) 7.21-7.40 (br, 6H, *Ar*), 7.71-7.80 (br, 2H, *Ar*) 7.90 (d, 1H, *6-H* (pyridinone)). ^{13}C NMR ($CDCl_3$, 500 MHz) δ (ppm) 12.4, 29.5, 50.6, 62.4, 73, 117.4, 123.8, 125.5, 127.73, 128, 128.2, 129.1, 130.2, 132.3, 133.1, 137.4, 138.4, 142.6, 148.30, 164.9, 173. MS: *m/z* 443 $[M]^+$.

3-(3- (benzyloxy) -2 -methyl-4- oxopyridin-1(4H)-yl) propyl 2-chlorobenzoate (7b)

Light brownish oil; yield 0.71 g (43%); IR (cm^{-1}): 1728 (ester C=O stretch), 1625 (ketone C=O stretch), 1379 (C-N stretching), 1249-1292 (C-O stretching), 3064 (aromatic C-H stretching), 833 and 875 (aromatic weak CH out-of-plane bending modes) 2854-2926 **(**C-H, aliphatic, stretching), 1514 (C=C, aromatic, bending), ^{1}H NMR ($CDCl_3$, 500 MHz) δ (ppm) 2.11 (m, 5H, N-CH_2*CH_2*CH_2O and *2-CH_3*), 4.00 (t, 2H, N*CH_2*CH_2), 4.32 (t, 2H, CH_2*CH_2*O), 5.21 (s, 2H,*CH_2*ph), 6.71 (d, 1H, *5-H* (pyridinone)), 7.31-7.50 (br, 9H, *Ar*), 7.81 (d, 1H, *6-H* (pyridinone)). ^{13}C NMR ($CDCl_3$, 500 MHz) δ (ppm) 12.4, 29.8, 50.8, 61.6, 73, 117.4, 126.8, 128, 128.2, 129.1, 129.6, 131.2, 131.5, 133, 136.2, 137.4, 138.3, 140.9, 146, 165.5, 173.1. MS: *m/z* 411 $[M]^+$.

3- (3- (benzyloxy) -2-methyl-4- oxopyridin-1(4H)-yl) propyl 3-chlorobenzoate (7c)

Light brownish oil; yield 0.77 g (46%); IR (cm^{-1}):1722 (ester C=O stretch, 1625 (ketone C=O stretch), 1379 (C-N stretching), 1253-1286 (C-O stretching), 3064 (aromatic C-H stretching), 833 and 877 (aromatic weak CH out-of-plane bending modes), 2854-2947 **(**C-H, aliphatic, stretching), 1517 (C=C, aromatic, bending). ^{1}H NMR ($CDCl_3$, 500 MHz) δ (ppm) 2.11 (m, 5H, N-CH_2*CH_2*CH_2O and *2-CH3*), 3.51 (t, 2H, N*CH2*CH_2), 4.00 (t, 2H, CH_2*CH_2*O), 5.22 (s, 2H,*CH_2*ph),6.51 (d, 1H, *5-H* (pyridinone), 7.32-7.52 (br, 7H, *Ar*), 7.61 (d, 1H, *Ar*, H-*meta* to the carboxyl group), 7.91 (d, 1H, *Ar*, H-*ortho* to the carboxyl group), 8.00 (d, 1H *6-H*(pyridinone)). ^{13}C NMR ($CDCl_3$, 500 MHz) δ (ppm) 12.3, 29.8, 50.5, 61.5, 72.9, 117.4, 127.6, 128, 128.2, 129, 129.5, 131.2, 133.3, 134.6, 137.4, 138.2, 140.6, 146.1, 164.9, 173.2. MS: *m/z* 411 $[M]^+$.

3-(3- (benzyloxy) -2-methyl- 4-oxopyridin-1(4H)-yl) propyl 4-chlorobenzoate (7d)

Light brownish oil; yield 0.74 g (45%); IR (cm^{-1}): 1712 (ester C=O stretch), 1624 (ketone C=O stretch), 136 (C-N stretching), 1261-1280 (C-O stretching) 1593 (shouldered, aromatic C=C bending), 3066 (aromatic C-H stretching), 844 and 879 (aromatic weak CH out-of-plane bending modes), 2854-2947 (C-H, aliphatic, stretching), 3429 (intermolecular hydrogen bonding), 1519 (C=C, aromatic, bending). ^{1}H NMR ($CDCl_3$, 500 MHz) δ (ppm) 2.22 (m, 2H, N-CH_2*CH_2* CH_2O), 2.52 (s, 3H, *2-CH3*), 4.31 (t, 2H, N*CH2*CH_2), 4.53 (t, 2H, CH_2*CH_2*O), 5.01 (s, 2H,*CH_2*ph), 7.41-7.52 (br, 6H, *Ar* and *5-H* (pyridinone)) 7.62 (d, 2H, *Ar*, H-*meta* to the carboxyl group), 7.90 (d, 2H, *Ar*, H-*ortho* to the carboxyl group), 8.43 (d, 1H, *6-H*(pyridinone)). ^{13}C NMR (DMSO-d_6, 500 MHz) δ (ppm) 13.4, 28.9, 53.5, 62.5, 74.3, 113.4, 128.7, 128.8, 128.9, 129, 129.3, 131.5, 136.7, 138.8, 142.4, 143.6, 148.9, 165.2, 173.3. MS: *m/z* 411 $[M]^+$.

3-(3-(benzyloxy)-2-methyl-4-oxopyridin-1(4H)-yl) propyl 4-methylbenzoate (7e)

Light brownish oil; yield 0.76 g (48%); IR (cm^{-1}): 1714 (ester C=O stretch), 1622 (ketone C=O stretch), 1247-1274 (C-O stretching), 3061 (aromatic C-H stretching), 837 (aromatic weak CH out-of-plane bending modes), 2854-2924 **(**C-H, aliphatic, stretching), 3415 (intermolecular hydrogen bonding). ^{1}H NMR ($CDCl_3$, 500 MHz) δ (ppm) 2.00 (br, 5H, N-CH_2*CH_2*CH_2O and 2-CH3), 2.41 (m, 3H, *para CH3* to the carboxyl group), 4.00 (t, 2H, N*CH2*CH_2), 4.31 (t, 2H, CH_2*CH_2*O), 5.23 (s, 2H,*CH_2*ph), 6.63 (d, 1H, *5-H* (pyridinone)) 7.21-7.40 (br, 9H, *Ar*) 7.91 (d, 1H, *6-H* (pyridinone)). ^{13}C NMR ($CDCl_3$, 500 MHz) δ (ppm) 12, 29.7, 50.7, 61, 73, 117.5, 125.9, 126.6, 128, 128.2, 129.5, 130.1, 137.3, 137.5, 137.8, 139.5, 140, 144.2, 152.1, 166.2, 173.2. MS: *m/z* 391 $[M]^+$.

3- (3- (benzyloxy)-2-methyl -4-oxopyridin-1(4H)-yl) propyl 4-bromobenzoate (7f)

Light brownish oil; yield 1.07 g (58%); IR (cm^{-1}): 1720 (ester C=O stretch), 1624 (α, β-unsaturated ketones C=O stretch) 3023-3062 (aromatic =C-H stretching), 1587 (C-C stretch in-ring), 1253-1271 (C-O stretching), 588 (C-Br stretching), 1398 (C-N stretching), 2924-2954 **(**C-H, aliphatic stretching), 3437 (intermolecular hydrogen bonding). ^{1}H NMR ($CDCl_3$, 500 MHz) δ (ppm) 2.01 (m, 5H, N-CH_2*CH_2*CH_2O and 2-CH_3), 3.92 (t, 2H, N*CH2*CH_2), 4.33 (t, 2H, CH_2*CH_2*O), 5.23 (s, 2H,*CH_2*ph), 6.42 (d, 1H, *5-H* (pyridinone), 7.23-7.44 (br, 7H, *Ar*), 7.66 (d, 2H, *Ar*, H-*meta* to the carboxyl group), 7.94 (d, 1H *6-H* (pyridinone)). MS: *m/z* 457 $[M]^+$.

3- (3- (benzyloxy)-2- methyl -4-oxopyridin-1(4H)-yl) propyl 2-nitrobenzoate (7g)

Light brownish oil; yield 0.57 g (33%); IR (cm^{-1}):1732 (ester C=O stretch, 1624 (ketone C=O stretch), 1253-1290 (C-O stretching), 3064 (aromatic C-H stretching), 839 (aromatic weak CH out-of-plane bending modes), 2852-2922 **(**C-H, aliphatic, stretching), 3427 (intermolecular hydrogen bonding), 1352 and 1533 (symmetric and asymmetric stretch respectively of the NO_2 group). ^{1}H NMR ($CDCl_3$, 500 MHz) δ (ppm) 2.00 (br, 5H, N-CH_2*CH_2*CH_2O and 2-CH3), 3.82 (t, 2H, N*CH_2*CH_2), 4.33 (t, 2H, CH_2*CH_2*O), 5.23 (s, 2H,*CH_2*ph), 6.44 (d, 1H, *5-H* (pyridinone)), 7.25-7.45 (br, 6H *Ar* and, H-*ortho* to the carboxyl group), 7.73-7.82 (br, 3H, H-*meta* and *para* to the carboxyl group), 7.92 (d,1H, *6-H* (pyridinone)). ^{13}C NMR ($CDCl_3$, 500 MHz) δ (ppm) 12.3, 29.5, 50.5, 62.4, 72.9, 117.5, 123.8, 126.7, 127.9, 128.2, 129, 130.1, 132.3, 133.1, 137.5, 138.3, 140.6, 146.1, 148.2, 164.9, 173.2. MS: *m/z* 422 $[M]^+$.

Table 1. The inhibitory activity of the synthesized compounds **7a-7h**.

Compounds	Absorption of compounds Mean ± SD	Absorption of Heme Mean ± SD	Absorption difference	Heme inhibition (%)
7a	0.174 ± 0.002	0.054 ± 0.001	0.12	39
7b	0.18 ± 0.009	0.051 ± 0.0006	0.129	34
7c	0.14 ± 0.005	0.062 ± 0.001	0.078	49
7d	0.32 ± 0.006	0.113 ± 0.002	0.207	45
7e	0.244 ± 0.02	0.054 ± 0.001	0.19	4
7f	0.148 ± 0.015	0.055 ± 0.001	0.093	53
7g	0.21 ± 0.018	0.054 ± 0.0007	0.156	1
7h	0.212 ± 0.05	0.056 ± 0.002	0.156	20
Chloroquine	0.245 ± 0.022	0.085 ± 0.002	0.160	93

3- (3- (benzyloxy)-2-methyl- 4-oxopyridin-1(4H)-yl) propyl 4-nitrobenzoate (7h)

Light brownish oil; yield 0.51 g (30%); IR (cm^{-1}):1726 (ester C=O stretch), 1616 (ketone C=O stretch), 1570 (shouldered, aromatic C=C bending), 1246-1274 (C-O stretching), 3111 (aromatic C-H stretching), 850 (aromatic weak CH out-of-plane bending modes), 2854-2924 **(**C-H, aliphatic, stretching), 3415 (intermolecular hydrogen bonding), 1348 and 1525 (symmetric and asymmetric stretch respectively of the NO_2 group). ^{1}H NMR ($CDCl_3$, 500 MHz) δ (ppm) 2.10 (br, 5H, N-CH_2*CH_2*CH_2O and 2-CH3), 3.90 (t, 2H, N*CH2*CH_2), 4.33 (t, 2H, CH_2*CH_2*O), 5.25 (s, 2H,*CH_2*ph), 6.42 (d, 1H, *5-H* (pyridinone)), 7.23-7.47 (br, 7H *Ar* and, H-*ortho* to the carboxyl group), 8.13 ((d, 2H, H-*meta* to the carboxyl group), 8.34 (d, 1H, *6-H* (pyridinone)). ^{13}C NMR ($CDCl_3$, 500 MHz) δ (ppm) 12.4, 29.7, 50.6, 62.1, 73, 117.5, 123.7, 128, 128.2, 129, 130.6, 131.3, 134.7, 137.4, 138.1, 140.5, 150.7, 164.3, 173. MS: *m/z* 422 $[M]^+$.

Bioassay protocol

β-hematin screening

The synthesized compounds **7a**, **7b**, **7c**, 7d, **7e**, **7f**, **7g**, and **7h** were tested for activity against the formation of β-hematin, a synthetic form of heme detoxification biomineral, hemozoin. The results were shown as the percentage of heme detoxification inhibition and polymerization. The assay results were deemed positive if the percentage of inhibition was more than 90%, while less than 90% were illustrated as negative results. The screening value of all target compounds has been shown in Table 1.

Cytotoxic effects of synthesized compounds

All of the synthesized compounds were evaluated for their antiproliferative effects against PC12 and fibroblast cell lines *via* MTT assay. As Fig. 1A and B show the growth inhibitory of the target compounds were evaluated on the PC12 and fibroblast cell lines.

Cell uptake assay

According to gained results of the MTT method, **7a**, **7b**, **7c**, **7d**, **7e,** and **7f**, were selected to detect cellular uptake potential by PC12 cells. Because of the fluorescent feature of these compounds, staining them was not required. The cellular uptake efficiency at 100 µg/mL of the abovementioned compounds was evaluated upon 24 h incubation of PC12 cells. Obtained images of fluorescent microscope revealed the cellular uptake potential of all target compounds (Fig. 2) with a sharp blue emission to treated cells indicating both monitoring characterization and anticancer power of them. Obtained images of fluorescent microscope manifested that all the compounds possessed halogen and methyl had emission in cellular uptake.

Molecular docking study

The Gold algorithm and Gold score fitness of synthetic compounds that contain π-alkyl, π-π stacking, and Fe…C are illustrated in Table2. Interaction of some compounds (**7c**, **7d**, **7f,** and chloroquine) with the heme sheet is shown in Fig. 3.

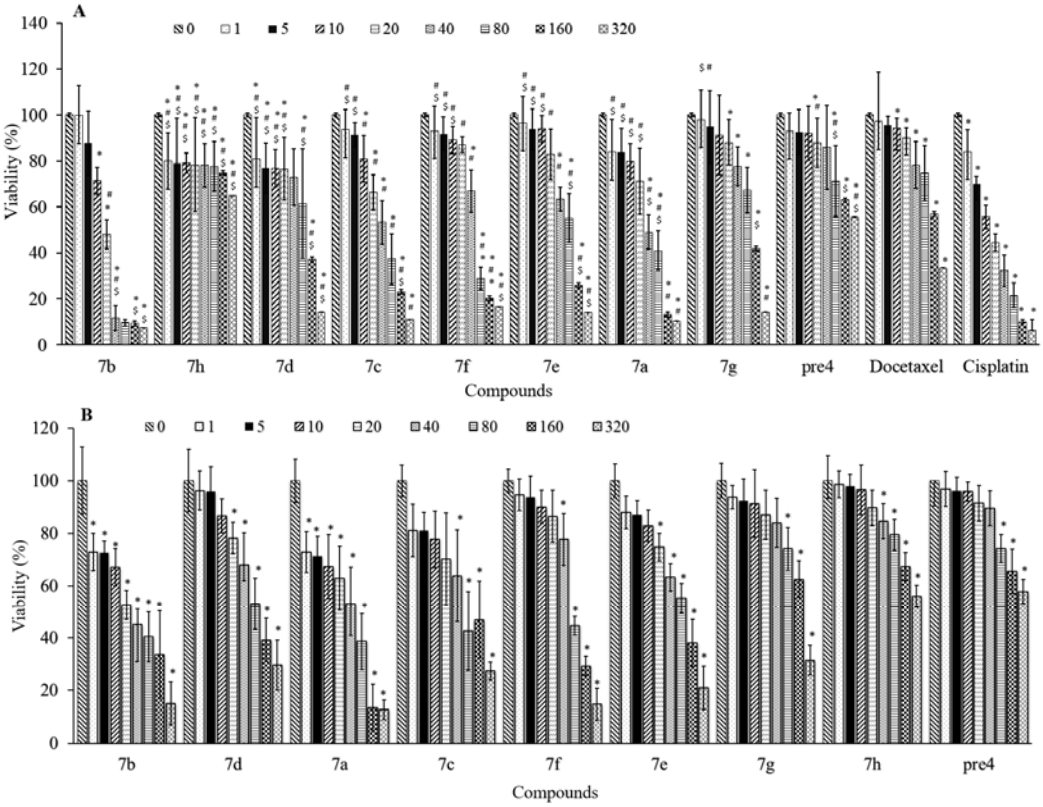

Fig. 1. Toxicity effects of target compounds against (A) PC12 cell line *via* MTT assay and (B) fibroblast cell line *via* MTT assay. Each value represents mean ± SEM. All experiments were done in triplicate. $^{*}P < 0.05$ Indicates significant differences compared to the 0 concentration (negative control) corresponding to each compound, $^{\#}P < 0.05$ versus docetaxel, and $^{\$}P < 0.05$ against cisplatin.

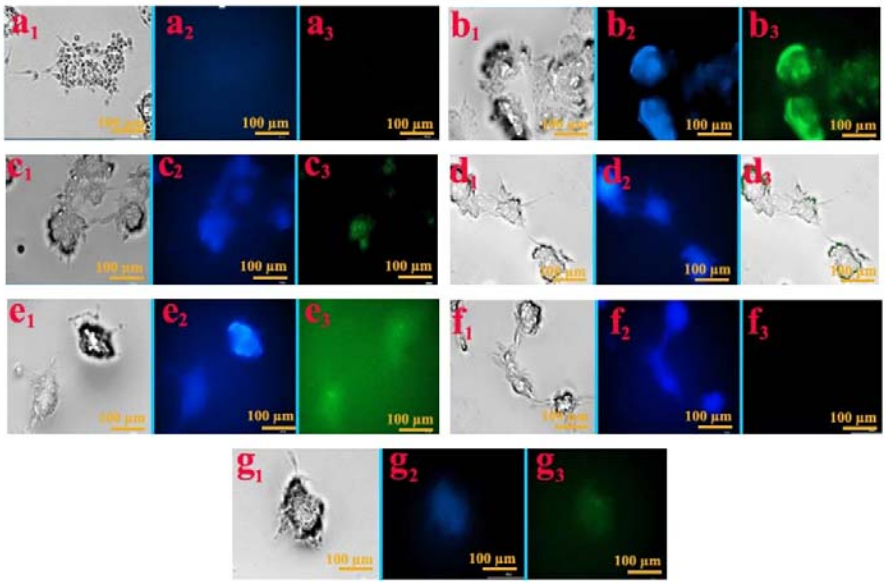

Fig. 2. Fluorescent microscopy of PC12 cells after 24-h incubation with synthesized compounds at 37 °C. The cellular uptake was visualized by overlaying images obtained by bright field, GFP, and DAPI emissions: left image from bright field; middle images from DAPI, and right images from GFP emissions. a-g are contributed to non-treated cells, **7b, 7c, 7d, 7f, 7e, 7a** compounds, respectively. GFP, Green fluorescent protein; DAPI, 4′,6-diamidino-2-phenylindole.

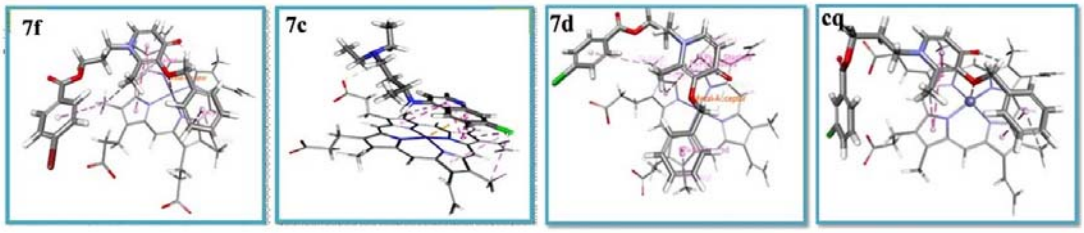

Fig. 3. Predicted binding mode of **7f**, **7c**, **7d,** and **cq** compounds with heme sheet by docking procedure.

Table 2. GOLD docking score for each synthesized compound.

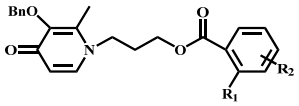

Entry	R1	R2	GOLD fitness score
7a	Cl	Cl	44.37
7b	Cl	H	42.00
7c	H	meta-Cl	41.32
7d	H	para-Cl	44.37
7e	H	para-Me	41.42
7f	H	para-Br	50.24
7g	NO2	H	44.19
7h	H	para-	50.28
Chloroquine			48.58

DISCUSSION

Maltol was chosen for the synthesis 4-pyridinones core, associated with minimal toxicity and facility for synthetic manipulation. All of pyridinones derivatives were prepared through several steps according to Scheme 1. Firstly 3-hydroxyl group of maltol was O-benzylated through Williamson ether synthesis. This step is responsible for protecting, increasing lipophilicity, and interplaying with the π system of the porphyrin ring (28). In the next step, an aliphatic linker was introduced to the structure through Aza-Michael addition which not only converts pyran-4-one core to pyridinone-4-one but creates a site to continue the structure. In this reaction, a catalyst is often used to remove the proton. The catalytic role of NaOH can be replaced by increasing the reflux temperature up to 150 °C. The obtained compound of this stage (**4**), in the presence of triethylamine, was reacted with different benzoyl chloride derivatives to produce the final products (**7a-7h**). It should be noted that benzoyl chloride derivatives were obtained from the reaction of various benzoic acids with thionyl chloride which is an excellent chlorine reagent. Since resonance contributions are deemed far superior for nitrogen than oxygen, pyridinone-4-one has emission fluorescence compared with pyran-4-one (29).

The synthesized compound was structurally confirmed with FT-IR, NMR, and MS techniques (the results are presented in the experimental part).

As seen in the IR spectra, in the reaction of known compound **3** with aliphatic amino alcohol linker, the formation of hydroxyl peak in region 2329 cm^{-1} as well as stretching aliphatic hydrogen peaks in 2873-2924 cm^{-1} confirm the structure of compound **4**. Then, in the reaction of benzoyl chloride derivatives with compound **4**, the disappearance of the hydroxy peak in 2329 cm^{-1} and the appearance of the new carbonyl peak in the region of 1712-1732 cm^{-1} confirm the formation of the final esteric structures.

The NMR spectral data of the synthesized products recorded in $CDCl_3$ along with its possible assignments was reported in the experimental part. The chemical shift of NCH_2CH_2 was seen as a triplet peak at 3.5 ppm in compound **4** which was shifted to around 4 ppm in final products. Similarly, the peak related to CH_2CH_2O which was observed as a triplet peak at 3.9 ppm in compound **4,** appeared in 4.2-4.3 ppm as a result of the esteric group in the final products. The protons related to $N\text{-}CH_2CH_2CH_2O$ were overlapped with 2-CH_3 in targeted derivatives and appeared in the multiple peaks around 2.2 ppm. The OH peak of the alcoholic intermediate which was observed at 3.6 ppm was disappeared in the target compounds. As ^{13}C NMR indicated, peaks around 170 and 164 ppm were assigned to C=O bonds of ketone and ester, respectively.

Aromatic C=C atoms were observed close to 128.2-148.4 ppm. C2-C5 was seen at 113-130 ppm. CH2ph was shown around 73 ppm and aliphatic C-C atoms were observed in 30-60 ppm. The chemical shift around 12 ppm supports 2-CH_3 assignment. To summarize, the NMR spectra showed characteristic peaks for the synthesized compounds. The molecular mass of the compounds was also confirmed by MS analysis and given in the experimental part.

However, all compounds showed less β-hematin inhibition activity than the positive control (chloroquine), according to the biological results. Among the mentioned compounds, more activity in β-hematin inhibition belonged to the **7f**, **7c,** and **7d** compounds which showed about 50% activity in β-hematin inhibition. Therefore **7f**, **7c,** and **7d** were considered more potent regarding β-hematin inhibition among the studied compounds. It is remarkable to say *para* substitutions of Br on the aromatic ring (**7f**) showed better inhibition activity than other compounds. These results revealed that substitution of Cl and Br atoms (negative inductive effect and positive mesomeric effect) on *para* and *meta* positions increased inhibition activity (30). The substitution of Cl on *meta* position (**7c**) was a little more active than *para* position (**7d**). Compound **7a** with two Cl atoms on *ortho* and *para* positions showed activity middle of compounds **7b** and **7d,** this is probably due to the unfavorable *ortho* position for Cl substitutions. Replacement of methyl as a short-chain aliphatic with a weak electron-donating group (31) in the *para* position of aromatic ring caused a significant reduction in potency of the **7e** compound. The o-/*p*-NO_2 substituted led to increasing polarity and unfavorable *in vitro* activity, however, **7h** was more active than **7g**. For the **7g** compound, in addition, *ortho*-substitution of the NO_2 group did not seem appropriate as well. The better β-hematin inhibition activity of **7f**, **7c**, and **7d** compounds might be attributed to π-π stacking, π-alkyl of benzyloxy with the porphyrin rings in heme sheets. Moreover, since that O in the benzylic substitution, Cl and Br as metal acceptors contributed to the favorable result in β-hematin inhibition, as previous studies have shown (20), such interactions can be effective in β-hematin inhibition.

Among synthesized compounds, the highest inhibitory effect against PC12 was related to **7b** with the IC_{50} of 18 µg. The IC_{50} of **7a**, **7c**, **7d**, **7e**, **7f**, **7g**, as well as cisplatin and docetaxel as positive controls against PC12 were 37, 43, 77, 83, 60, 180, 8, and 280 µg/mL, respectively. The **7h** and alcoholic precursor didn't display remarkable toxicity in defined concentrations. IC_{50} of **7a**, **7b, 7c**, **7d**, **7e**, **7f**, and **7g** on fibroblast cell line were 44, 26, 59, 85, 95, 71 and 190 µg/mL, respectively. **7h** did not show acceptable growth-inhibitory impact for the determination of IC_{50} at applied concentrations (Fig. 1b). Regarding the obtained results, it can be found that **7a**, **7b, 7c**, **7d**, **7e**, and **7g** could be better cytotoxic agents, respectively.

All synthesized compounds except **7h** showed higher potency compared to docetaxel as a positive control against PC12. As seen from the results, cytotoxicity of targeted molecules is directly related to drug lipophilicity which is a key factor in transport across the biological membranes (32). The structure-activity relationship indicated that bulky lipophilic and also *ortho*, *meta*, and *para* substitution with halogen atoms led to better activity than the other compounds. The *o*-Cl substituted, (**7b**) compound demonstrated excellent potency (about 16 folds more potent) than docetaxel. The *meta*-Cl substituted led to a decrease in the effect of **7c** (2 folds less potent than **7b** compound). The **7d** compound showed nearly 2 folds less potent than the **7c** compound. It seemed potency of **7a** compound with a double Cl on *ortho* and *para* position was almost in the middle of 3 compounds mentioned above, this result confirmed that *para* substitution led to decrease or complete loss of activity. It is worth pointing out that *para* substitution of Br (**7f**) has a remarkable effect on the potency that originated from one more electron shell compared with the Cl atom and increased the lipophilicity. The **7e** compound was about 2-fold more potent than docetaxel, this result disclosed that cytotoxicity was alleviated by the replacement of *para*-methyl substitution. Although the NO_2 imposed a lot of polarity on compound **7g** and reduced hydrophobic interactions, it showed one fold and half

potency against PC12 to the replacement of nitro in the *ortho* position. This result strongly confirmed the importance of *ortho*-substitution. It is desirable to note that, not only NO_2 was not a suitable functional group, but also *para* substitution led to a decrease of potency for compound **7h**.

The most effective compound in cancer treatment (**7b**) had the most emission in cellular uptake. Probably in this compound the interaction of carbonyl group with Br facilitated singlet-to-triplet conversion *via* so- named heavy-atom- effect, and resulted in more emission of **7f** versus compound **7e** (32). Fluorescence quenching effect being remarkable for the bromide, negligible for chloride led to intersystem crossing to dark triplet states and decline of the fluorescence intensity. Two heavy atoms of Cl could significantly reduce the fluorescence intensity for compound **7a**. The quenching of fluorescence for compounds **7g** and **7h** was attributed to the quenching ability of the electronegative NO_2 groups (32).

The synthesized esteric derivatives of pyridinone were docked into the heme and compared with chloroquine binding mode as a positive control. Recent research has proven the π-π stacking between benzyloxy group of compounds with the porphyrin ring which would play an influential role in inhibition (33,34). Benzyloxy and benzoate ring and also hydrophobic R1 and R2 substitution in these compounds established π-π stacking interaction with porphyrin ring. Similar to the β-hematin inhibition assay, among the synthesized compounds **7f** is one of the potent compounds in interaction with the heme sheet.

Briefly in this study, cytotoxic assay, cell uptake, and β-hematin inhibition bioassay revealed that synthesized compounds in addition to their moderate ability to inhibition of heme polymerization, had acceptable cytotoxic activity, like chloroquine, quinoline caffeic acid, and ethyl ester of caffeic acid which possess antimalarial and significant anticancer activity (35). So, this study introduced novel compounds that could be antimalarial and/or anticancer agents through a further study on these compounds.

CONCLUSION

In conclusion, we synthesized a small library of novel benzyloxy-4-oxopyridin benzoate derivatives. All compounds were characterized by IR, ^{1}H NMR, ^{13}C NMR, and mass spectral data and evaluated for β-hematin inhibition. **7f**, **7c,** and **7d** showed moderate ability in β-hematin inhibition. These results revealed that substitution of Cl and Br atoms (negative inductive effect and positive mesomeric effect) on *para* and *meta* positions increased inhibition activity. The molecular docking study showed **7h** and **7f** had effective interactions with the heme sheet through hydrophobic interaction. The MTT assay of targeted compounds verified the cytotoxic properties of the synthesized compounds. The results showed that bulky lipophilic and also *ortho, meta,* and *para* substitution with halogen atoms led to better activity than the other compounds. The best cytotoxic compound (**7b**) showed more activity compared with docetaxel. Cell uptake results also confirmed the potential of the synthesized compounds as an interpolative agent. These results revealed that further study on these compounds can lead to exploring compounds that can be considered anti-malarial or cytotoxic agents.

Acknowledgments

The authors would like to thank Dr. Mahsa (Masoumeh) Mohammadi for the precise reading of the manuscript and thankful the Research Council of Kermanshah University of Medical Sciences and Vice-chancellery for Research of Isfahan University of Medical Sciences for peace of mind feedback provided and financial support of this work (Grant No. 397786).

Conflict of interest statement

The authors declared no conflicts of interest in this study.

Authors' contributions

L. Saghaie conceived and supervised the project; M. Mohebi performed the experiments, analyzed and interpreted the data; S. Esmaeili, F. Bagheri, and A. Aliabadi advised the

biological study of compounds; N. Fayazi and M. Rostami assisted in the docking study and synthesis of compounds, respectively; P. Asadi helped in writing the manuscript. The final version of the manuscript was approved by all authors.

REFERENCES

1. Chong CR, Sullivan DJ. Inhibition of heme crystal growth by antimalarials and other compounds: implications for drug discovery. Biochem Pharmacol. 2003;66(11):2201-2212. DOI: 10.1016/j.bcp.2003.08.009.
2. Perez BC, Tixeira C, Figueiras M, Gut J, Rosenthal PJ, Gomes JRB, *et al*. Novel cinnamic acid/4-aminoquinoline conjugates bearing non-proteinogenic amino acids: towards the development of potential dual action antimalarials. Eur J Med Chem. 2012;54:887-899. DOI: 10.1016/j.ejmech.2012.05.022.
3. Belete TM. Recent progress in the development of new antimalarial drugs with novel targets. Drug Des Devel Ther. 2020;14:3875-3889. DOI: 10.2147/DDDT.S265602.
4. Egan TJ. Haemozoin formation. Mol Biochem Parasitol. 2008;157(2):127-136. DOI: 10.1016/j.molbiopara.2007.11.005.
5. Fong KY, Wright DW. Hemozoin and antimalarial drug discovery. Future Med Chem. 2013;5(12):1437-1450. DOI: 10.4155/fmc.13.113.
6. Phi LTH, Sari IN, Yang YG, Lee SH, Jun N, Kim KS, *et al*. Cancer stem cells (CSCs) in drug resistance and their therapeutic implications in cancer treatment. Stem Cells Int. 2018;2018:5416923. DOI: 10.1155/2018/5416923.
7. Kamaludin NF, Zakaria SA, Awang N, Mohamad R, Pim NU. Cytotoxicity assessment of organotin(IV) (2-metoxyethyl) methyldithiocarbamate compounds in human leukemia cell lines. Orient J Chem. 2017;33(4):1756-1766. DOI: 10.13005/ojc/330420.
8. Alama A, Viale M, Cilli M. *In vitro* cytotoxic activity of tri-*n*-butyltin(IV)lupinylsulfide hydrogen fumarate (IST-FS 35) and preliminary antitumor activity *in vivo*. Invest New Drugs. 2009;27:124-130. DOI: 10.1007/s10637-008-9148-x.
9. Ito H. The formation of maltol and isomaltol through degradation of sucrose. Agric Biol Chem. 1977;41:1307-1308. DOI: 10.1080/00021369.1977.10862669.
10. Yellamma K, Jyothi P. *In silico* approach for validation of maltol derivatives as acetylcholinesterase inhibitors. Int J Pharm Sci Rev Res. 2017;42(1):300-306.
11. Perokovic VP, Car Z, Usenik A, Opacak-Bernardi T, Juric A, Tomic S. Adamantyl pyran-4-one derivatives and their *in vitro* antiproliferative activity. Mol Diversity. 2020;24:253-263. DOI: 10.1007/s11030-019-09948-1.
12. Jiang X, Guo J, Lv Y, Yao C, Zhang Ch, Mi Z, *et al*. Rational design, synthesis and biological evaluation of novel multitargeting anti-AD iron chelators with potent MAO-B inhibitory and antioxidant activity. Bioorg Med Chem. 2020;28(12):115550. DOI: 10.1016/j.bmc.2020.115550.
13. Pergola PE, Kopyt NP. Oral ferric maltol for the treatment of iron-deficiency anemia in patients with CKD: a randomized trial and open-label extension. Am J Kidney Dis. 2021;78(6):846-856.e1. DOI: 10.1053/j.ajkd.2021.03.020.
14. Sabet R, Fassihi A, Hemmateenejad B, Saghaei L, Miri R, Gholami M. Computer-aided design of novel antibacterial 3-hydroxypyridine-4-ones: application of QSAR methods based on the MOLMAP approach. J Comput Aided Mol Des. 2012;26(3):349-361. DOI: 10.1007/s10822-012-9561-2.
15. Heppner DG, Kontoghiorghes G, Kontoghiorghes GJ, Eaton JW. Antimalarial properties of orally active iron chelators. Blood. 1988;72(1):358-361. PMID: 3291984.
16. Jiang X, Zhou T, Bai R, Xie Y. Hydroxypyridinone-based iron chelators with broad-ranging biological activities. J Med Chem. 2020;63(23):14470-14501. DOI: 10.1021/acs.jmedchem.0c01480.
17. Li W, Su X, Han Y, Xu Q, Zhang J, Wang Z, *et al*. Maltol, a Maillard reaction product, exerts anti-tumor efcacy in H22 tumor-bearing mice *via* improving immune function and inducing apoptosis. RSC Adv. 2015;5:101850-101859. DOI: 10.1039/C5RA17960B.
18. Reddy VD, Dayal D, Szalda DJ, Cosenza SC, Reddy MVR. Syntheses, structures, and anticancer activity of novel organometallic ruthenium-maltol complexes. J Organomet Chem. 2012;700:180-187. DOI: 10.1016/j.jorganchem.2011.12.011.
19. Kandioller W, Hartinger CG, Nazarov AA, Kasser J, John R, Jakupec MA, *et al*. Tuning the anticancer activity of maltol-derived ruthenium complexes by derivatization of the 3-hydroxy-4-pyrone moiety. J Organomet Chem. 2009;694:922-929. DOI: 10.1016/j.jorganchem.2008.10.016.
20. Fayyazi N, Esmaeili S, Taheri S, Ribeiro FF, Scotti MT, Scotti L, *et al*. Pharmacophore modeling, synthesis, scaffold hopping and biological β-Hematin inhibition interaction studies for anti-malaria compounds. Curr Top Med Chem. 2019;19(30):2743-2765. DOI: 10.2174/1568026619666191116160326.
21. Andayi WA, Egan TJ, Chibale K. Kojic acid derived hydroxypyridinone-chloroquine hybrids: synthesis, crystal structure, antiplasmodial activity and β-haematin inhibition. Bioorg Med Chem Lett. 2014;24(15):3263-3267. DOI: 10.1016/j.bmcl.2014.06.012.
22. Andayi WA, Egan TJ, Gut J, Rosenthal PJ, Chibale K. Synthesis, antiplasmodial activity, and β-hematin inhibition of hydroxypyridone-chloroquine hybrids. ACS Med Chem Lett. 2013;4(7):642-646. DOI: 10.1021/ml4001084.

23. Rablen PR. Is the acetate anion stabilized by resonance or electrostatics? A systematic structural comparison. J Am Chem Soc. 2000;122(2):357-368. DOI: 10.1021/ja9928475.
24. Beddard G, Carlin S, Harris L, Porter G, Tredwell C. Quenching of chlorophyll fluorescence by Nitrobenzene. Photochem Photobiol. 1978;27(4):433-438. DOI: 10.1111/j.1751-1097.1978.tb07625.x.
25. Chernysheva MV, Bulatova M, Ding X, Haukka M. Influence of substituents in the aromatic ring on the strength of halogen bonding in iodobenzene derivatives. Cryst Growth Des. 2020;20:7197-7210. DOI: 10.1021/acs.cgd.0c00866.
26. Salvatella L. The alkyl group is a –I + R substituentEl grupo alquilo es un sustituyente –I + R. Educación Química. 2017;28(4):232-237. DOI: 10.1016/j.eq.2017.06.004.
27. Priimagi A, Cavallo G, Metrangolo P, Resnati G. The halogen bond in the design of functional supramolecular materials: recent advances. Acc Chem Res. 2013;46(11):2686-2695. DOI: 10.1021/ar400103r.
28. Sciortino A, Pecorella R, Cannas M, Messina F. Effect of halogen ions on the photocycle of fluorescent carbon nanodots. C J Carbon Res. 2019;5(4):64-73. DOI: 10.3390/c5040064.
29. Hameed A, Masood S, Hameed A, Ahmed E, Sharif A, Abdullah MI. Anti-malarial, cytotoxicity and molecular docking studies of quinolinyl chalcones as potential anti-malarial agent. J Comput Aided Mol Des. 2019;33(7):677-688. DOI: 10.1007/s10822-019-00210-2.
30. Alson SG, Jansen O, Cieckiewicz E, Rakotoarimanana H, Rafatro H, Degotte G, *et al*. *In-vitro* and *in-vivo* antimalarial activity of caffeic acid and some of its derivatives. J Pharm Pharmacol. 2018;70(10):1349-1356. DOI: 10.1111/jphp.12982 .
31. Serafim TL, Carvalho FS, Marques MP, Calheiros R, Silva T, Garrido J, *et al*. Lipophilic caffeic and ferulic acid derivatives presenting cytotoxicity against human breast cancer cells. Chem Res Toxicol. 2011;24(5):763-764. DOI: 10.1021/tx200126r.
32. Sheikhmoradi V, Saberi S, Saghaei L, Pestehchian N, Fassihi A. Synthesis and antileishmanial activity of antimony (V) complexes of hydroxypyranone and hydroxypyridinone ligands. Res Pharm Sci. 2018;13(2):111-120. DOI: 10.4103/1735-5362.223793.
33. Ugarte-Uribe B, Perez-Rentero S, Lucas R, Avinno A, Reina JJ, Alkorta I, *et al*. Synthesis, cell-surface binding, and cellular uptake of fluorescently labeled glucose-DNA conjugates with different carbohydrate presentation. Bioconjug Chem. 2010;21(7):1280-1287. DOI: 10.1021/bc100079n.
34. Momany FA, Rone R. Validation of the general purpose QUANTA® 3.2/CHARMm® force field. J Comput Chem. 1992;13(7):888-900. DOI: 10.1002/JCC.540130714.
35. Ghasemi JB, Aghaee E, Jabbari A. Docking, CoMFA and CoMSIA studies of a series of N-benzoylated phenoxazines and phenothiazines derivatives as antiproliferative agents. Bull Korean Chem Soc. 2013;34(3):899-906. DOI: 10.5012/bkcs.2013.34.3.899.